Bioorganic Chemistry

DOI: 10.1002/anie.200906294

In Vivo Chemistry for Pretargeted Tumor Imaging in Live Mice**

*Raffaella Rossin, Pascal Renart Verkerk, Sandra M. van den Bosch, Roland C. M. Vulders, Iris Verel, Johan Lub, and Marc S. Robillard**

Bio-orthogonal chemical reactions between two exogenous moieties in living beings are sought after tools that have powerful applications in chemical biology, molecular imaging, and medicine.[1–4] The exquisite selectivity of these reactions—the Staudinger ligation and the strain-promoted azide-alkyne cycloaddition—has been exploited for the metabolic labeling and subsequent tagging and visualization of biomolecules in mice by using ex vivo detection,[1–3] and in live zebrafish embryos.[4] However, the reaction kinetics ($k_2 \leq 7.6 \times 10^{-2}\,\text{M}^{-1}\text{s}^{-1}$) have required a high dose and large excess of secondary reagent to achieve detectable binding. Applications in molecular imaging and medicine that require low doses and semi-equimolar conditions have therefore remained unrealized. Reactions that retain selectivity but have faster kinetics could extend in vivo chemistry to clinically relevant procedures in mammalian disease models, by allowing the intravenous administration of a small amount of probe to non-invasively delineate low-abundance species. The rapid blood clearance and excretion typical of most small to medium-sized molecules necessitates that the reaction occurs within minutes. Such selectivity and effective equimolar reactivity has never been demonstrated in a living animal.

A prominent application that would greatly benefit from the introduction of a rapid bio-orthogonal reaction is pretargeted radio-immunoimaging and radio-immunotherapy, namely, tumor targeting of a monoclonal antibody (mAb) followed by binding of a small radiolabeled probe to the tumor-bound mAb.[5] The superior image contrast and the ability to administer higher (therapeutic) radiation doses compared to directly labeled mAbs is offset by the drawbacks of the current biological pretargeting systems, such as immunogenicity (streptavidin systems) or the need to re-engineer the parent mAb (bispecific antibodies).[5,6] A chemical pretargeting approach would in principle allow universal and straightforward tagging and in vivo tracking of mAbs, mAb fragments, or other proteins without severe perturbation of their in vivo properties.

The fast reaction kinetics and selectivity in vitro of the inverse-electron-demand Diels–Alder reaction between electron-deficient tetrazine and strained *trans*-cyclooctene (TCO) derivatives[7] suggest potential for effective use at the low concentrations of tumor antigens. The cycloaddition of olefins with tetrazines affords an intermediate, which then rearranges by expulsion of dinitrogen in a retro-Diels–Alder cycloaddition to form a stable dihydropyridazine conjugate (Figure 1). It was unknown if the Diels–Alder components could also contend with the more-demanding conditions in vivo, such as side reactions and metabolism as well as prolonged residence times and the corresponding required stability. We thus designed a novel tumor pretargeting approach based on the Diels–Alder reaction between tetrazine-DOTA derivative **1** radiolabeled with ^{111}In and TCO **2** conjugated to anti-TAG72 mAb CC49 through the lysine residue (Figures 1 and 2). The TAG72 antigen was selected because of its limited internalization and shedding as well as its overexpression in a wide range of solid tumors, including colorectal cancer.[8]

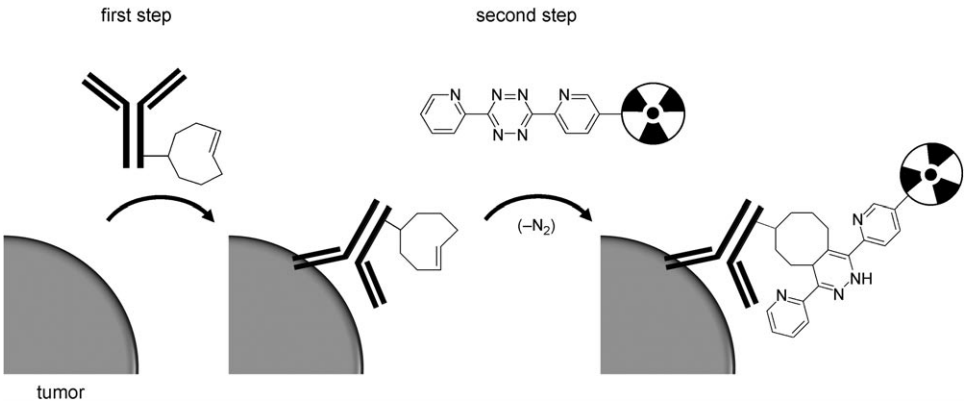

Figure 1. General scheme of tumor pretargeting by using the inverse-electron-demand Diels–Alder reaction.

On the basis of the in vitro kinetics ($k_2 = 2000\,\text{M}^{-1}\text{s}^{-1}$, methanol/water (9:1)) and stability reported by Fox and coworkers[7] for an electron-deficient bis(pyridino)-1,2,4,5-tet-

[*] Dr. R. Rossin, P. Renart Verkerk, S. M. van den Bosch, R. C. M. Vulders, Dr. I. Verel, Dr. J. Lub, Dr. M. S. Robillard
Biomolecular Engineering, Philips Research
High Tech Campus 11, 5656 AE Eindhoven (The Netherlands)
Fax: (+31) 40-2744-906
E-mail: marc.robillard@philips.com

[**] We thank Prof. H. Grüll for discussions and support, C. van Kammen (Maastricht University), C. van Helvert (Maastricht University), M. Berben, and S. Kivits for assistance with animal experiments, Dr. D. Burdinski for discussions, and Dr. W. ten Hoeve (Syncom) for synthesis of the precursors.

Supporting information for this article is available on the WWW under http://dx.doi.org/10.1002/anie.200906294.

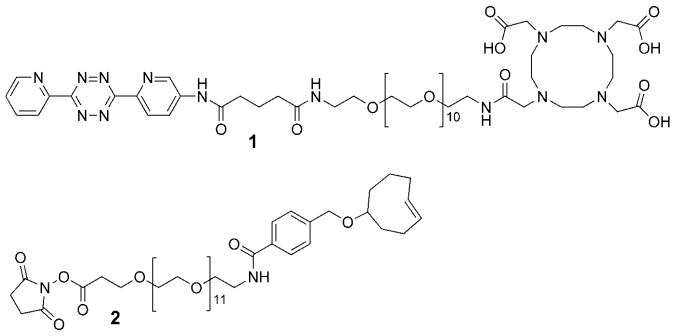

Figure 2. Pretargeting components: tetrazine-DOTA (**1**) and *trans*-cyclooctene-NHS (**2**).

razine, we postulated that **1** should possess optimal reactivity with TCO, combined with sufficient stability during its projected short residence time in vivo in our pretargeting experiments. In anticipation of a large increase of the reaction rate in more aqueous media, we studied the kinetics of radiolabeled **1** with CC49-TCO in phosphate-buffered saline (PBS) and found a second order rate constant of $13090 \pm 80\,\mathrm{M^{-1}s^{-1}}$ at 37 °C (complete reaction within 3 minutes at 1.67 μM; see Figure S9 in the Supporting Information).[9]

Our investigations continued with determination of the stability and reactivity of the two components in biological media. In vitro assays in PBS, serum, and blood showed (Table 1) that [^{111}In]-**1** should be stable for the duration of its presence in mice (blood clearance half-life of 9.8 minutes; see Figure S13 in the Supporting Information). We observed a fast reaction between [^{111}In]-**1** and CC49-TCO in vitro in semi-equimolar conditions and at low concentration (3.3 μM) within 10 minutes in PBS, serum and blood (Table 2). The yields obtained from the reactions with 10 and 15 equivalents of [^{111}In]-**1** indicated the presence of an average of 7.4 reactive TCO moieties per antibody. Furthermore, the nonspecific binding of [^{111}In]-**1** to unmodified CC49 or other media constituents was found to be very low. To assess the stability of the mAb-bound TCO moiety in vivo we treated mice with CC49-TCO and then treated extracted blood samples ex vivo with an excess of tetrazine **1**. The reaction yield, corrected for CC49-TCO blood clearance, revealed that 75 % of the CC49-bound TCO present in blood was still reactive after 24 hours circulation, thus indicating good in vivo stability.

To test the Diels–Alder reaction in living animals we administered CC49-TCO to mice bearing colon cancer xenografts, followed one day later with injection of 3.4 equivalents of [^{111}In]-**1** with respect to TCO. The chemically tagged tumors reacted rapidly with [^{111}In]-**1**, resulting in pronounced localization of radioactivity in the tumor, as demonstrated by single photon emission computed tomography/computed tomography (SPECT/CT) imaging of live mice three hours after injection (Figure 3 a,d; see movie S1 in the Supporting Information). The SPECT quantification (see Table S3 in the Supporting Information) of the tumor gave 4.2 % injected dose per gram (% ID g^{-1}) and a tumor-to-muscle ratio (T/M) of 13.1:1. We also observed limited uptake in blood and nontarget tissues, such as the liver, which we attributed to

Table 1: In vitro stability of [^{111}In]-**1**.[a]

Incubation *t* [h]	PBS[b]	Serum[b]	Blood[c]
1	98.2 ± 0.7	93.5 ± 0.4	78.0
2	96.7 ± 0.3	86.8 ± 1.1	59.0
20	64.4 ± 1.1	20.1 ± 2.7	11.0

[a] Data normalized to 100 % at $t = 0$ and presented as mean ± standard deviation. [b] $n = 3$. [c] $n = 1$.

Table 2: In vitro reactions to determine the stoichiometry between [^{111}In]-**1** (three concentrations) and CC49-TCO (3.3 μM) after 10 min incubation at 37 °C; reaction yields in % based on [^{111}In]-**1**.[a]

	PBS[b]	Serum[b]	Blood[c]
1 equiv	85.6 ± 1.3 (0.9 ± 0.0)	88.3 ± 1.8 (0.9 ± 0.0)	87.0 (0.9)
10 equiv	74.7 ± 6.9 (7.5 ± 0.7)	72.0 ± 1.3 (7.2 ± 0.1)	72.6 (7.3)
15 equiv	50.0 ± 1.5 (7.5 ± 0.2)	48.5 ± 0.4 (7.3 ± 0.1)	50.0 (7.5)
control[d]	0.3 ± 0.3	0.2 ± 0.2	0.0

[a] Parentheses: number of tetrazine probes bound per CC49. Data are presented as mean ± standard deviation. Equivalents of [^{111}In]-**1** with respect to CC49. [b] $n = 3$. [c] $n = 1$. [d] Reaction between unmodified CC49 (3.3 μM) and [^{111}In]-**1** (15 equiv).

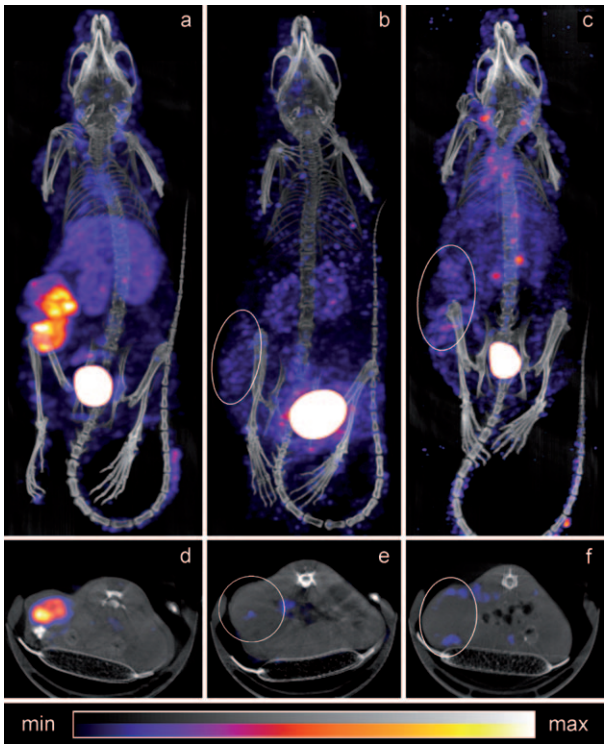

Figure 3. Small-animal SPECT/CT imaging of live mice bearing colon carcinoma xenografts: posterior projections of mice preinjected with a) CC49-TCO (100 μg) followed one day later by [^{111}In]-**1** (25 equiv to CC49; 3.4 equiv to TCO, 42 MBq), b) CC49 (100 μg) followed one day later by [^{111}In]-**1** (same amount as in (a), 20 MBq), and c) Rtx-TCO (100 μg) followed one day later by [^{111}In]-**1** (same amount as in (a), 50 MBq); d)–f) single transverse slices (2 mm) passing through the tumors in (a)–(c).

reaction with residual circulating CC49-TCO. Besides the tumor, the bulk of the radioactivity was found in the bladder, and some residual activity was visible in the kidney (Figure 3a, see movie S1 in the Supporting Information). Importantly, the tumor could not be discriminated from the surrounding tissue in mice treated with unmodified CC49 (Figure 3b, e; 0.3% ID g^{-1}, T/M = 0.5:1). Almost no radioactivity was retained in the blood and nontargeted organs, as the probe was again rapidly eliminated through the urinary tract, thus signifying its bio-orthogonality. Mice treated with TCO-modified rituximab (Rtx), which lacks specificity for TAG72, showed the expected retention of [^{111}In]-**1** in blood and nontarget organs, and a significantly reduced accumulation in the tumor (Figure 3c, f; 1.0% ID g^{-1}, T/M = 2.1:1). The high-resolution postmortem image (see movie S2 in the Supporting Information) shows ^{111}In activity in the aorta and carotid arteries as well as in the retroorbital regions. The rim of the tumor is also visible, because of extensive vascularization, whereas the rest of the tumor is devoid of radioactivity.

Next, we studied the distribution and specific colocalization of both pretargeting components through corresponding dual isotope biodistribution experiments with ^{125}I-labeled mAbs (CC49-TCO, CC49, or Rtx-TCO) and [^{111}In]-**1** (Figure 4). Residual ^{125}I-mAbs were detectable in blood and in blood-rich organs such as the heart and lung 27 hours after injection, and showed the typical distribution pattern of long-circulating antibodies (Figure 4a).[10] Both CC49 and CC49-TCO accumulated efficiently in tumors, with tumor-to-blood ratios (T/B) around 3:1 (Figure 4c) and high T/M ratios (Figure 4d). Considerably lower accumulation in the tumor, accompanied by a T/B ratio lower than 1:1 was found for Rtx-TCO (Figure 4c), thereby supporting the antigen-specific binding of CC49-TCO.

The [^{111}In]-**1** biodistribution data confirmed the [^{111}In]-**1** SPECT images. In the mice pretreated with CC49-TCO or Rtx-TCO, the distribution of [^{111}In]-**1** mirrored that of the mAbs (Figure 4a–d). For example, a fivefold higher uptake of [^{111}In]-**1** was found in the tumors containing [^{125}I]CC49-TCO compared to [^{125}I]Rtx-TCO. Almost no ^{111}In uptake was detected in the blood and in most tissues of the group pretreated with unmodified [^{125}I]CC49. Importantly, whilst the uptake of [^{125}I]CC49 by the tumors was the highest among the three groups, the ^{111}In uptake by the tumors in this same group was 16 times lower than that in the [^{125}I]CC49-TCO group. In all mice, the kidney exhibited a relatively high uptake of ^{111}In as a consequence of [^{111}In]-**1** excretion. The finding that the tetrazine accumulated only in tissues containing a TCO-modified species verified that a chemical reaction between these two entities occurred in vivo. Calculation of the absolute amounts of TCO and tetrazine present in tissues from the % ID g^{-1} values of ^{125}I and ^{111}In revealed a remarkable 57% (in blood) and 52% (in tumor) reaction yield between TCO and tetrazine moieties,[11] at TCO concentrations of 0.4 nmol g^{-1} (blood) up to 0.9 nmol g^{-1} (in tumor), and max 2.1 nmol g^{-1} for the tetrazine (Figure 4e). It is noteworthy that this high reaction yield and corresponding tumor contrast were achieved in the complex interior of a mouse in a reaction time of minutes, limited by the 9.8 minute circulation half-life of [^{111}In]-**1**.

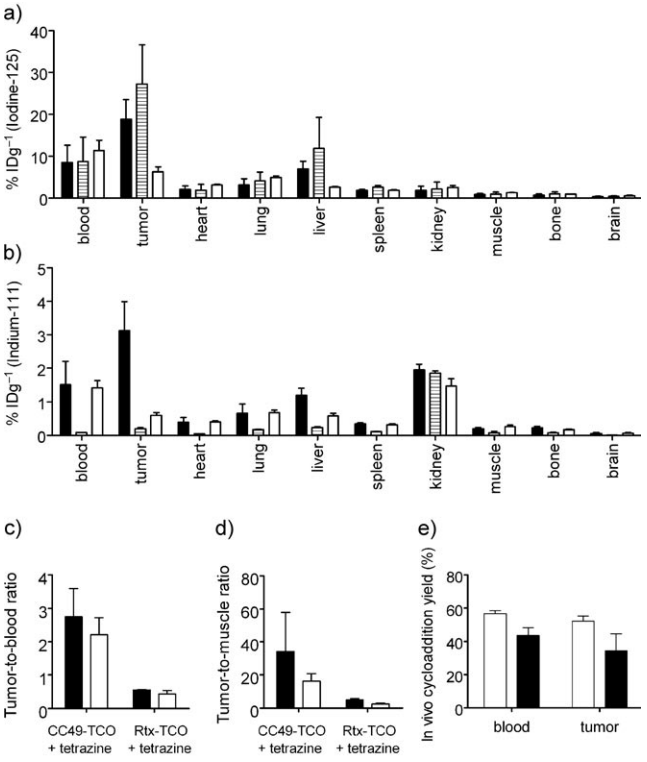

Figure 4. Dual isotope biodistribution experiment: a) uptake of [^{125}I]CC49-TCO, [^{125}I]CC49, and [^{125}I]Rtx-TCO in selected organs 27 hours after intravenous injection; b) uptake of [^{111}In]-**1** 3 hours after injection and 27 hours after injection of ^{125}I-mAbs (solid bars: [^{125}I]CC49-TCO + [^{111}In]-**1**; striped bars: [^{125}I]CC49 + [^{111}In]-**1**; empty bars: [^{125}I]Rtx-TCO + [^{111}In]-**1**); c) tumor-to-blood and d) tumor-to-muscle ratios in mice administered with [^{125}I]CC49-TCO or [^{125}I]Rtx-TCO followed one day later by [^{111}In]-**1** (solid bars: ^{125}I-data; empty bars: ^{111}In-data); e) reaction yields between TCO and tetrazine **1** in blood and tumor in living mice (empty bars: [^{125}I]CC49-TCO + [^{111}In]-**1**; solid bars: [^{125}I]Rtx-TCO + [^{111}In]-**1**). Data are presented as mean ± standard deviation (n = 3).

In summary, we have demonstrated the first use of a bio-orthogonal chemical reaction between two exogenous moieties in living animals for the non-invasive imaging of low-abundance targets under clinically relevant conditions. Intravenous administration of a small, semi-equimolar amount (nanomol) of a rapidly excreted probe convincingly delineated a tumor-bound antibody in a high chemical yield, despite the challenging pharmacokinetic constraints of a mammalian disease model. The inverse-electron-demand Diels–Alder reaction, therefore, has the potential to improve the state of the art of pretargeting, because it circumvents the use of immunogenic (strept)avidin systems and the protein engineering techniques used for bispecific antibodies. Current efforts are directed towards reducing the amount of free-circulating CC49-TCO to increase the tumor-to-blood ratio of [^{111}In]-**1** in preparation for radiotherapy studies with tumor-bearing mice. Finally, this reaction may serve as a point of entry for a wider range of chemical applications in living systems.

Experimental Section

See the Supporting Information for the synthesis and characterization of tetrazine-DOTA (**1**) and TCO-NHS (**2**), and for other detailed procedures. All animal experiments were approved by the ethical review committee of the Maastricht University Hospital (the Netherlands), and were performed according to the principles of laboratory animal care (NIH publication 85–23, revised 1985), and the Dutch national law "Wet op de Dierproeven" (Stb 1985, 336).

Received: November 8, 2009
Revised: December 16, 2009
Published online: April 12, 2010

Keywords: antibodies · cancer · Diels–Alder reaction · molecular imaging · radiochemistry

[1] J. A. Prescher, D. H. Dube, C. R. Bertozzi, *Nature* **2004**, *430*, 873 – 877.
[2] D. H. Dube, J. A. Prescher, C. N. Quang, C. R. Bertozzi, *Proc. Natl. Acad. Sci. USA* **2006**, *103*, 4819 – 4824.
[3] J. M. Baskin, J. A. Prescher, S. T. Laughlin, N. J. Agard, P. V. Chang, I. A. Miller, A. Lo, J. A. Codelli, C. R. Bertozzi, *Proc. Natl. Acad. Sci. USA* **2007**, *104*, 16793 – 16797.
[4] S. T. Laughlin, J. M. Baskin, S. L. Amacher, C. R. Bertozzi, *Science* **2008**, *320*, 664 – 667.
[5] D. M. Goldenberg, R. M. Sharkey, G. Paganelli, J. Barbet, J. F. Chatal, *J. Clin. Oncol.* **2006**, *24*, 823 – 834.
[6] D. M. Goldenberg, E. A. Rossi, R. M. Sharkey, W. J. McBride, C. H. Chang, *J. Nucl. Med.* **2008**, *49*, 158 – 163.
[7] M. L. Blackman, M. Royzen, J. M. Fox, *J. Am. Chem. Soc.* **2008**, *130*, 13518 – 13519.
[8] J. Schlom, D. Eggensperger, D. Colcher, A. Molinolo, D. Houchens, L. S. Miller, G. Hinkle, K. Siler, *Cancer Res.* **1992**, *52*, 1067 – 1072.
[9] During the completion of our studies, a lower in vitro reactivity for a more stable system was reported, see: N. K. Devaraj, R. Upadhyay, J. B. Haun, S. A. Hilderbrand, R. Weissleder, *Angew. Chem.* **2009**, *121*, 7147 – 7150; *Angew. Chem. Int. Ed.* **2009**, *48*, 7013 – 7016.
[10] C. A. Boswell, M. W. Brechbiel, *Nucl. Med. Biol.* **2007**, *34*, 757 – 778.
[11] Corrected for non-specific accumulation; not corrected for TCO degradation.

